The Astronomical Journal, 153:19 (10pp), 2017 January doi:10.3847/1538-3881/153/1/19

THE *HUBBLE SPACE TELESCOPE* UV LEGACY SURVEY OF GALACTIC GLOBULAR CLUSTERS. VIII. PRELIMINARY PUBLIC CATALOG RELEASE

M. Soto[1,2], A. Bellini[1], J. Anderson[1], G. Piotto[3,4], L. R. Bedin[4], R. P. van der Marel[1], A. P. Milone[5], T. M. Brown[1], A. M. Cool[6], I. R. King[7], A. Sarajedini[8], V. Granata[3,4], S. Cassisi[9], A. Aparicio[10,11], S. Hidalgo[10,11], S. Ortolani[3,4], and D. Nardiello[3,4]

[1] Space Telescope Science Institute, San Martin Drive 3700, Baltimore, MD 21218, USA; mario.soto@uda.cl
[2] Universidad de Atacama, Departamento de Física, Copayapu 485, Copiapó, Chile
[3] Dipartimento di Fisica e Astronomia Galileo Galilei, Università di Padova, Vicolo dell'Osservatorio 3, I-35122 Padova, Italy
[4] INAF-Osservatorio Astronomico di Padova, Vicolo dell'Osservatorio 5, I-35122 Padova, Italy
[5] Research School of Astronomy and Astrophysics, The Australian National University, Cotter Road, Weston, ACT, 2611, Australia
[6] Department of Physics and Astronomy, San Francisco State University, 1600 Holloway Avenue, San Francisco, CA 94132, USA
[7] Department of Astronomy, University of Washington, Box 351580, Seattle, WA 98195-1580, USA
[8] Department of Astronomy, University of Florida, 211 Bryant Space Science Center, Gainesville, FL 32611, USA
[9] Osservatorio Astronomico di Teramo, Via Mentore Maggini s.n.c., I-64100 Teramo, Italy
[10] Instituto de Astrofísica de Canarias, E-38200 La Laguna, Tenerife, Canary Islands, Spain
[11] Department of Astrophysics, University of La Laguna, E-38200 La Laguna, Tenerife, Canary Islands, Spain
Received 2015 December 15; revised 2016 October 31; accepted 2016 November 1; published 2016 December 21

ABSTRACT

The *Hubble Space Telescope (HST) UV Legacy Survey of Galactic Globular Clusters* (GO-13297) has been specifically designed to complement the existing F606W and F814W observations of the Advanced Camera for Surveys (ACS) Globular Cluster Survey (GO-10775) by observing the most accessible 47 of the previous survey's 65 clusters in three WFC3/UVIS filters F275W, F336W, and F438W. The new survey also adds super-solar metallicity open cluster NGC 6791 to increase the metallicity diversity. The combined survey provides a homogeneous 5-band data set that can be used to pursue a broad range of scientific investigations. In particular, the chosen UV filters allow the identification of multiple stellar populations by targeting the regions of the spectrum that are sensitive to abundance variations in C, N, and O. In order to provide the community with uniform preliminary catalogs, we have devised an automated procedure that performs high-quality photometry on the new UV observations (along with similar observations of seven other programs in the archive). This procedure finds and measures the potential sources on each individual exposure using library point-spread functions and cross-correlates these observations with the original ACS-Survey catalog. The catalog of 57 clusters we publish here will be useful to identify stars in the different stellar populations, in particular for spectroscopic follow-up. Eventually, we will construct a more sophisticated catalog and artificial-star tests based on an optimal reduction of the UV survey data, but the catalogs presented here give the community the chance to make early use of this *HST* Treasury survey.

Key words: globular clusters: general – Hertzsprung–Russell and C–M diagrams – stars: Population II – techniques: photometric

1. INTRODUCTION

Early in the 20th century, Harlow Shapley used the distribution of globular clusters (GCs) to determine the extent of the Milky Way (Shapley 1918) and the Sun's position in it to overturn the most accepted model of the Galaxy at the time, the Kapteyn universe. Nowadays, GCs are still recognized as an important component of Galactic structure and hold important clues for numerous questions related to stellar evolution, stellar dynamics, variable and binary stars, and the conditions present during the formation of the Milky Way itself. Consequently, over the years, important efforts have been made to construct complete GC catalogs and thus address some of these questions (e.g., Shapley 1930; Arp 1965; Webbink 1985; Djorgovski & King 1986; Djorgovski & Meylan 1993; Harris 1996). However, many of the properties included in these catalogs were obtained from integrated light or small stellar samples, and that necessarily constrained the scope of resulting science to general parameters such as total brightness, colors, metallicities, and reddenings. In addition, many of the early catalogs were limited by the inhomogeneity that results from different instruments and set-ups.

GC surveys based on homogeneous data sets are highly desirable since that facilitates comparisons such as those involving age or horizontal-branch morphology. Initial attempts to provide homogenous samples, such as those of Rosenberg et al. (2000), which produced a catalog of 56 clusters using ground-base data, and Piotto et al. (2002), which sampled the cores of 74 clusters using Wide Field Planetary Camera 2 (WFPC2), hinted at what such homogeneous data sets could do. It was only natural that *Hubble Space Telescope*'s (*HST*) Advanced Camera for Surveys (ACS) would contribute the most uniform, homogeneous catalog to date in the ACS Globular Cluster Survey (GO-10775; Sarajedini et al. 2007 and Anderson et al. 2008). This survey improved considerably on many of the limitations of previous surveys, which typically suffered from crowding in the central regions or uneven sampling (e.g., the differences between the PC and the WF chips in the WFPC2). The legacy value of the ACS Globular Cluster Survey (henceforth ACS GCS) has been demonstrated by studies addressing a broad range of topics related to GCs, such as mass functions (Paust et al. 2010), horizontal-branch morphologies (Dotter et al. 2010; Milone et al. 2014), relative ages (Marín-Franch 2009; VandenBerg

et al. 2013), the Sagittarius dwarf spheroidal galaxy nucleus (Siegel et al. 2007), stellar evolution tracks and isochrones (Dotter et al. 2007), relative ages of GCs (De Angeli et al. 2005), clusters with multiple sequences (e.g., NGC 1851; Milone et al. 2008; Piotto et al. 2012, 2015), and mass segregation (Goldsbury et al. 2013).

Even at the time of the ACS GCS, GCs were largely assumed to be the quintessential examples of simple stellar populations, born in a single starburst episode. Anderson (1997), Lee et al. (1999), and Bedin et al. (2004) provided the first counter-example to this rule by showing that the main-sequence of ω Centauri was divided into at least two distinct sequences. Even though hints of this had been seen spectroscopically and photometrically along the red giant branch (RGB), the main-sequence data showed that this was not simply an artifact of atmospheric evolutionary mixing.

This initial discovery was soon followed by evidence of multiple populations (MPs) in other GCs: NGC 2808 (D'Antona et al. 2005; Piotto et al. 2007), NGC 6441 (Gratton et al. 2006; Bellini et al. 2013), NGC 1851 (Cassisi et al. 2008; Milone et al. 2008), NGC 6388 (Carretta et al. 2007; Bellini et al. 2013; Piotto et al. 2015); NGC 6121 (M4; Marino et al. 2008), NGC 6656 (M22; Marino et al. 2009), NGC 104 (47 Tuc; Anderson et al. 2009; Milone et al. 2012), NGC 6752 (Milone et al. 2010, 2013), NGC 2419 (Di Criscienzo et al. 2011), and NGC 288 (Piotto et al. 2013). In many cases the detection of the MPs was made through the Na–O anti-correlation that stems from the CNO-cycle processed differences of second generation (2G) stars compared with first generation (1G) stars (Milone et al. 2013). The filters F275W, F336W, and F438W of the Wide Field Camera 3 (WFC3) in its ultraviolet-visible (UVIS) channel happen to be particularly sensitive to these differences. While F275W covers the OH molecular band, F336W includes an NH band, and F438W CN and CH bands. Hence, 1G stars are C- and O-rich and N-poor and tend to be faint in F275W and F438W, while remaining bright in F336W. On the contrary, 2G stars are C- and O-poor and N-rich and tend to be bright in F275W and F438W, but faint in F336W (Milone et al. 2012). Since this filter set is so perfectly suited to study MPs (as well as many other cluster phenomena), the *Hubble Space Telescope UV Legacy Survey of Galactic Globular Clusters* (GO-13297, PI-Piotto), was designed to use these filters in order to complement the existing optical-based ACS GCS.

Piotto et al. (2015) describe the motivation and observing strategy for the survey and show some preliminary results in terms of color–magnitude diagrams (CMDs). The current paper will provide a preliminary catalog of the survey results. It is organized as follows: in Section 2 we describe the WFC3/UVIS observations that have been used to construct each cluster catalog. In Section 3, we give a detailed description of our procedure, including the detection and measuring processes as well as the cross-identification with the ACS GCS catalogs. We discuss the advantages and shortcomings of these preliminary catalogs in Section 4. Finally, Section 5 summarizes the current catalog and points to an upcoming final version.

2. OBSERVATIONS

As mentioned above, the GO-13297 UV survey has been designed primarily as a follow-on to the existing $F606W$ and $F814W$ observations of the ACS GCS (see Sarajedini et al. 2007). The ACS GCS sample of clusters was originally selected based on several criteria, the most important being proximity to the Sun and low reddening [$E(B-V) < 0.35$]. With one exception, we restricted our sample to the clusters observed in the ACS GCS, but had to exclude those that were either too distant or too reddened to make observations in the UV practical. We also excluded three of the clusters that had already been observed in the UVIS filters. In all, we included 47 of the 65 ACS GCS clusters and added NGC 6791, an old metal-rich open cluster that extends our multiple stellar population investigation to super-solar metallicity.

As described more fully in Piotto et al. (2015), the faintness of stars in the F275W band is the main limitation to the survey. It would be prohibitive to get S/N $\sim$ 10 for all stars in Sarajedini's survey in the UV bands, so we aimed simply to reach a minimum accuracy of 0.02 magnitude (or S/N $\gtrsim$ 50), in the F275W band down to the turnoff. A total of 131 orbits were allocated to this program: 15 clusters needed only 2 orbits to attain four exposures per band according to our specifications, 4 clusters required 3 orbits each, 8 clusters were observed in 4 orbits, 3 clusters had 5 orbits, 2 clusters required 6 orbits, while 2 others only had 1 orbit each in only two bands. The remaining 14 clusters are either too distant or too reddened to detect MPs for stars below the turn-off, so for them we assigned just 2 orbits to allow identification of the MPs in the evolved populations.

Previous programs with suitable WFC3/UVIS observations in F275W, F336W, and F438W have also contributed to the catalog we present here. Pilot MPs WFC3/UVIS programs GO-12311 (PI: G. Piotto), GO-12605 (PI: G. Piotto), and the programs with similar observations, GO-11633 (PI: R.M. Rich), GO-11729 (PI: J. Holtzman), GO-12008 (PI: A. Kong), GO-12746 (PI: A. Kong), and GO-12971 (PI: H. Richer), allowed the sample presented here to be expanded to 57 clusters with 5-band data.

In addition to these WFC3/UVIS observations, described above, parallel ACS field observations have also been carried out for each cluster in the F475W and F814W bands. These parallel observations were designed to overlap with archival data in the outer regions of each cluster as much as possible, thus providing the foundation for proper-motion studies at different radii for a significant number of these clusters. The catalog presented here will focus exclusively on the core region observed by WFC3/UVIS.

A detailed account of the exposures for each cluster can be found in Piotto et al. (2015). For convenience, we provide a brief summary in Table 1.

3. DETECTING AND MEASURING IN A COMMON FRAME

3.1. An Automated Reduction Pipeline

As was the case with the ACS GCS, the number of images used in this project and the desire for a homogeneous catalog necessitate the use of an automated reduction procedure. This pipeline has to be effective enough to find stars (while avoiding artifacts) and at the same time produce results with a quality comparable to the original ACS GCS catalogs. Below we describe the steps taken in order to accomplish this.

Table 1
Summary of Cluster Observations

Cluster	R.A.	Decl.	F275W	F336W	F438W	ΔEpoch (years)
NGC 0104	00:24:15	−72:05:47	2 × 323, 12 × 348	2 × 485, 2 × 580, 2 × 720		5.1
NGC 0288	00:52:45	−26:34:43	6 × 400	4 × 350	4 × 41	6.3
NGC 0362	01:03:14	−70:50:53	6 × 519	4 × 350	4 × 54	6.3
NGC 1261	03:12:16	−55:12:58	4 × 834, 4 × 855, 2 × 918	5 × 413	5 × 164	7.7
NGC 1851	05:14:06	−40:02:47	14 × 1288	4 × 453	2 × 140	5.7
NGC 2298	06:48:59	−36:00:19	4 × 848, 4 × 980	1 × 327, 4 × 350	5 × 134	7.9
NGC 2808	09:12:02	−64:51:33	12 × 985	6 × 650	6 × 97	7.5
NGC 3201	10:17:36	−46:24:44	4 × 754	4 × 310	1 × 60, 1 × 68	7.7
NGC 4590	12:39:27	−26:44:38	4 × 696	4 × 305	2 × 60	7.9
NGC 4833	12:59:33	−70:52:35	4 × 895, 4 × 936	4 × 350	4 × 135	7.7
NGC 5024	13:12:55	18:10:05	3 × 1729, 3 × 1830	3 × 433, 3 × 460	3 × 170, 3 × 178	7.9
NGC 5053	13:16:27	17:42:00	4 × 829, 2 × 854, 4 × 879	5 × 415	5 × 164	8.0
NGC 5272	13:42:11	28:22:31	6 × 415	4 × 350	4 × 42	6.2
NGC 5286	13:46:26	−51:22:27	2 × 668, 2 × 797	4 × 310	2 × 65	7.9
NGC 5466	14:05:27	28:32:04	4 × 865, 4 × 928	4 × 350	4 × 135	7.9
NGC 5897	15:17:24	−21:00:36	4 × 874, 4 × 926	4 × 350	4 × 138	8.0
NGC 5904	15:18:33	02:04:51	4 × 689	4 × 306	2 × 58	8.1
NGC 5927	15:28:00	−50:40:26	6 × 668	1 × 30, 5 × 310, 2 × 475	2 × 66	7.6
NGC 5986	15:46:02	−37:47:11	4 × 668, 2 × 745	6 × 300	3 × 60	8.3
NGC 6093	16:17:02	−22:58:30	10 × 855	5 × 657	5 × 85	6.2
NGC 6101	16:25:48	−72:12:07	4 × 851, 4 × 889, 2 × 940	5 × 415	5 × 165	7.8
NGC 6121	16:23:41	−26:30:50	10 × 380, 2 × 735, 2 × 808	4 × 300	2 × 66	6.9
NGC 6144	16:27:13	−26:01:24	4 × 748	4 × 304	2 × 61	8.0
NGC 6171	16:32:31	−13:03:13	4 × 895, 4 × 926	4 × 350	4 × 136	8.1
NGC 6205	16:41:41	36:27:40	6 × 427	4 × 350	4 × 46	6.1
NGC 6218	16:47:14	−01:56:54	2 × 714, 2 × 790	4 × 306	1 × 58, 1 × 66	7.9
NGC 6254	16:57:09	−04:06:01	2 × 713, 2 × 790	4 × 306	2 × 60	7.8
NGC 6304	17:14:32	−29:27:43	2 × 693, 2 × 800	4 × 304	2 × 60	7.8
NGC 6341	17:17:07	43:07:58	2 × 707, 2 × 819	4 × 304, 2 × 425	2 × 57	7.2
NGC 6352	17:25:29	−48:25:19	2 × 706, 2 × 800	4 × 311, 5 × 400, 1 × 410	1 × 58, 1 × 72	7.0
NGC 6362	17:31:54	−67:02:52	2 × 720, 2 × 829	4 × 323, 1 × 368, 5 × 450	2 × 67	6.6
NGC 6366	17:27:44	−05:04:47	2 × 713, 2 × 795	4 × 305	2 × 62	8.3
NGC 6388	17:36:17	−44:44:08	4 × 888, 2 × 961, 2 × 999	4 × 350	4 × 133	8.2
NGC 6397	17:40:35	−53:39:57	2 × 709, 2 × 752	4 × 310, 6 × 620	2 × 66	6.4
NGC 6441	17:50:13	−37:03:05	4 × 887, 4 × 928	4 × 350	4 × 123	8.0
NGC 6496	17:59:03	−44:15:57	2 × 707, 2 × 800	4 × 303	1 × 61, 1 × 73	7.8
NGC 6535	18:03:50	00:17:48	2 × 713, 2 × 793	1 × 253, 4 × 305, 5 × 400	2 × 62	6.8
NGC 6541	18:08:02	−43:42:53	2 × 708, 2 × 758	4 × 300	2 × 65	8.0
NGC 6584	18:18:37	−52:12:56	2 × 709, 2 × 795	4 × 312	2 × 62	7.6
NGC 6624	18:23:40	−30:21:39	2 × 707, 2 × 800	4 × 295	1 × 62, 1 × 81	7.8
NGC 6637	18:31:23	−32:20:53	4 × 887, 2 × 923, 2 × 933	4 × 350	2 × 120, 2 × 130	7.9
NGC 6652	18:35:45	−32:59:26	2 × 690, 2 × 775, 2 × 800	6 × 305	1 × 60, 1 × 69, 1 × 86	7.5
NGC 6656	18:36:24	−23:54:12	12 × 812	4 × 475	2 × 141	5.9
NGC 6681	18:43:12	−32:17:31	2 × 706, 2 × 800	4 × 294	1 × 66, 1 × 83	7.7
NGC 6715	18:55:03	−30:28:47	3 × 1751, 3 × 1916	3 × 433, 3 × 475	3 × 170, 3 × 190	7.7
NGC 6717	18:55:06	−22:42:05	6 × 686	6 × 311	3 × 60	8.2
NGC 6723	18:59:33	−36:37:56	4 × 693, 2 × 734	6 × 313	3 × 60	8.0
NGC 6752	19:10:54	−59:59:11	12 × 369	1 × 30, 2 × 500		4.7
NGC 6779	19:16:35	30:11:00	2 × 706, 2 × 800	4 × 295	1 × 64, 1 × 81	7.8
NGC 6791	19:20:52	37:46:18	4 × 700	4 × 297	2 × 65	9.2[a]
NGC 6809	19:39:59	−30:57:53	2 × 746	2 × 294	1 × 66	7.9
NGC 6838	19:53:46	18:46:45	2 × 750, 2 × 792	4 × 303	2 × 65	7.7
NGC 6934	20:34:11	07:24:16	2 × 792	2 × 304	1 × 70	7.5
NGC 6981	20:53:27	−12:32:14	2 × 693, 2 × 710	4 × 304	2 × 64	7.7
NGC 7078	21:29:58	12:10:00	3 × 615, 3 × 700	6 × 350	6 × 65	5.5
NGC 7089	21:33:27	00:49:23	2 × 676, 2 × 735, 2 × 785	6 × 313	2 × 62, 1 × 70	7.4
NGC 7099	21:40:22	−23:10:47	2 × 725	2 × 303	1 × 65	8.1

Notes. In addition to the GO-13297 exposures, this table includes the exposures from GO-12311 and GO-12605, the pilot studies in MPs using WFC3/UVIS. Similar observations in the archive from programs GO-11633, GO-11729, GO-12008, GO-12746, and GO-12971 have also been included. Exposure times are in seconds. ΔEpoch corresponds to the time elapsed between first- and second-epoch observations, namely the time baseline between the ACS GCS observations and the new UV WFC3/UVIS images.
[a] First epoch from GO-10265 (PI: T. Brown).

3.2. Preliminary Reduction Steps

All the WFC3/UVIS observations described in Table 1 have been processed using the same procedures in order to provide homogeneous photometry. WFC3/UVIS _flt images have been corrected for the effects of imperfect charge-transfer efficiency (CTE) using the parallelized version of the STScI publicly available FORTRAN code[12] (see Anderson & Bedin 2010 for a detailed description of the method). Stellar positions and fluxes for individual exposures were obtained using the program hst1pass, which is based on the publicly available routine img2xym_WFC0.9x10 (Anderson & King 2006) and will be made public along with a future paper (J. Anderson 2016, in preparation). The code goes through each exposure, pixel-by-pixel, and identifies as a potential source of interest every pixel that: (1) has at least 25 electrons of flux over sky in its brightest 2 × 2 pixels, and (2) is brighter than any other pixel within a radius of 3 pixels. It uses an appropriate library point-spread function (PSF) to measure a least-squares position for the source (under the assumption that it is a star), a flux (using the central 5 × 5 pixels and an aperture correction based on the star's location within its central pixel), and also a quality-of-fit metric (Anderson et al. 2008). Finally, the routine corrects the measured position for geometric distortion using the solution in Bellini et al. (2011), then uses the WCS header information to transform positions into a common frame (in this case, the ACS GCS frame for the cluster).

3.3. One-pass Photometry

A star must be detectable and measurable reliably on an individual exposure to be included in the present catalog. The one-pass nature of this preliminary reduction does not allow us to go as faint as we will eventually go in the final catalog. In the final catalog, we will find stars simultaneously on multiple exposures in multiple filters, then measure them with consistent positions simultaneously in all available exposures, thus allowing deeper photometry. Here, we will restrict ourselves to the stars that have at least $S/N \simeq 10$ in individual exposures. In addition, since we are not attempting a full reduction of GO-13297 at this time, we will simply cross-identify our starlists with the existing ACS GCS catalog.

The finding routine described above produces for each image a list of sources, and for each source it determines an x and y position in the raw detector coordinates, a pixel-area-corrected raw instrumental magnitude m, an instrumental magnitude m_{1000} that has been zeropointed to correspond to a 1000 s exposure, and a quality-of-fit metric q. The calibration of the instrumental m_{1000} magnitudes into VEGAMAG happens later in our procedure, as we will see in Section 3.5. The routine also uses a distortion solution and the WCS information in the image header to transform the observed coordinates into the ACS GCS frame for that cluster to facilitate cross-identification. We call this reference frame the (u, v) frame.

3.4. Cross-identification With the ACS GCS

The processing of the one-pass lists was performed by another routine, named uvm2collate, which will also be described in J. Anderson (2016, in preparation). In brief, this routine cross-correlates the starlist from each exposure with the Sarajedini catalog, while at the same time generating a representative stacked image in the reference frame for each filter.

On account of typical errors of ∼0.5 arcsec in the guide-star positions that affect the absolute astrometry of all *HST* frames, we cannot assume that the (u, v) positions constructed based on the WCS header of each image to be in the ACS GCS frame will automatically be perfectly aligned with the actual stars in the ACS GCS catalog. Thus, for each exposure, we take the (u, v) list and find the horizontal and vertical offsets that provide the most matches with the relatively bright stars in the ACS GCS catalog using a matching radius of 1.75 pixels. This generous radius makes our initial matching robust against small errors in the absolute rotation of the *HST* frame as well.

We then take this initial cross-identification and use a full six-parameter linear transformation to relate our new positions to the master frame. We compute residuals and iteratively reject the most discordant star until there are no stars with residuals greater than 0.25 pixel. We then use these final transformations to compute improved (u, v) positions for each cross-identified star. Figure 1 shows the distribution of offsets and orientation adjustments for the 780 images that were transformed in this process. The offset represents the typical pointing error resulting from imperfect guide-star positions. The prevailing orientation difference of $0\overset{\circ}{.}05$ reflects the fact that the rotation we adopted between the distortion-solution frame of Bellini et al. (2011) and the V2 axis was slightly off. This did not prevent all the stars from being properly matched, and it will be fixed by the time the hst1pass software is released.

Once the final transformation from each exposure into the reference frame has been established, we take the original loosely cross-identified list and determine improved reference-frame positions for each star. The routine then takes all the cross-identified stars and computes an average position (and an rms about that position) for each star in the GO-13297 data set and an average instrumental magnitude (and an rms about that magnitude) in each band, iteratively rejecting observations that are discordant at the 3-sigma level. The position that we compute here is not optimized for astrometry; to do that we would have to take more care in performing the transformations and would have to weight the observations according to signal-to-noise. Even with these caveats, the position should be accurate to at least the 0.1 pixel-level (5 mas, implying a proper motion error of about 0.6 mas yr^{-1}, with a time baseline of 7–9 years). This should enable cluster-field rejection, even though it is not adequate for a study of the internal motions. A high-precision internal-motion catalog will be constructed using the algorithm in Bellini et al. (2014), using all available observations.

3.5. Photometric Calibration

Thus far in the procedure, our photometry of the GO-13297 images has been kept in the raw, instrumental system in order to give us a direct idea of the intrinsic signal-to-noise of each measurement. We also retain the 1000 s exposure-time-zeropointed photometry to facilitate eventual absolute calibration. While the PSFs we used to measure the one-pass fluxes were normalized to correspond to the total within 10 pixels ($0\overset{''}{.}4$), there is distortion in the raw frames and thus there can be small offsets between our photometry and that produced on the drizzle products, which have been carefully calibrated to VEGAMAG zeropoints.

[12] http://www.stsci.edu/hst/wfc3/ins_performance/CTE

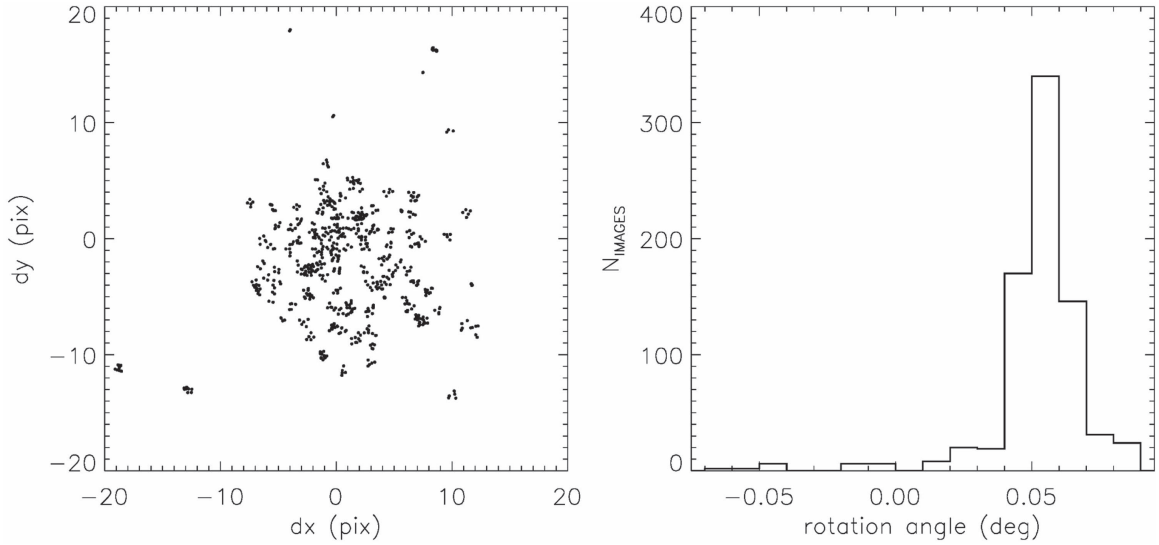

Figure 1. Left: distribution of offsets between our catalogs and the ACS GCS images derived from the 6-parameter linear transformations. Each point represents an exposure. The four-point clumpings reflect the fact that the dithered exposures in each visit tend to have the same guide-star related boresight offset. Right: histogram showing the distribution of relative rotation angle between our catalogs and the ACS GCS. The prevailing offset of 0.05° between the two frames indicates that our WFC3/UVIS distortion solution was not properly aligned with the V2 axis of the telescope. This will be improved before the release of the `hst1pass` software.

Therefore, in order to do the absolute calibration, we first had to reduce the DRZ images with aperture photometry using the standard 10-pixel-radius aperture, add the official zeropoints,[13] and the `_drz-aperture` corrections,[14] and cross-identify these stars with the ACS GCS master list in order to arrive at a calibrated magnitude (i.e., in VEGAMAG) for each star detected in each UVIS band. The next step was to determine a zeropoint for each filter.

The difference between our 1000-s-normalized magnitudes and the calibrated photometry should be a simple zeropoint that is the same for all clusters, since the process that goes from `_flt` to `_drz` is the same linear process for all images. Therefore, for ten representative clusters, we determined the offset between our photometry and the VEGAMAG photometry. Figure 2 shows the zeropoint determined for the three different filters for ten different clusters. The average zeropoint is noted at the top. We have used the average of the zeropoint correction for these ten clusters for the entire sample of 57 GCs.

3.6. Improvements to Come

It bears repeating that the catalog presented here is preliminary. It is based on a one-pass reduction with static library PSFs and it contains only those stars that were already found in Sarajedini's GC Treasury project. The CMDs shown in Piotto et al. (2015) and papers based on them are different from those that can be constructed from these catalogs, in that they are based on a more careful treatment of each cluster (including differential reddening corrections, custom PSF modeling for each exposure, UVIS-based star lists, etc.). All of these improvements will eventually be available for the final public catalog, but until all clusters can be reduced in the final optimal way, we decided to make this preliminary, uniformly reduced catalog available now. Section 5 will detail the anticipated improvements.

[13] http://www.stsci.edu/hst/wfc3/phot_zp_lbn

[14] http://www.stsci.edu/hst/wfc3/documents/handbooks/currentIHB/c06_uvis07.html

4. LEGACY PRODUCTS

The collation procedure described above operates on the list of stars in the original ACS GCS catalog for each cluster. It determines an average position for each star in the reference frame based on the observations from all the filters along with an average magnitude and rms about that magnitude for each star in each filter. It also reports for each filter the number of exposures in which a star could be found (`p`), the number of times it was found (`f`), and the number of times it was found consistently and not rejected (`g`).

4.1. Catalog Products

These quantities all come from the new GO-13297 data and are reported in the first 17 columns of our catalog for each cluster. Table 2 lists all the columns in our catalogs. For convenience, Columns 18 through 24 provide basic information from the ACS GCS to allow easy construction of five-band photometry and cluster-field separation proper motions. In columns 25 and 26 we list the displacements which we have rounded to 0.1 pixels.

Figure 3 shows an example of our catalog products for cluster NGC 6681. Panels (a) and (b) compare the positions of each star in the ACS GCS and the average position in our F275W, F336W, and F438W catalog, which reflects a time-baseline of ∼7–8 years. Panel (c) shows the CMD in our UV bands, while panel (d) shows the physical distribution of the stars in the ACS GCS reference frame.

In panel (b) we have drawn a square representing the expected astrometric accuracy of 0.1 pixel centered on the origin. Similarly, we have marked in panels (a) and (b) the stars outside a radius of 0.35 pixel as field stars (orange points). The same field stars have been highlighted in panels (c) and (d).

4.2. Image Products

In addition to producing the catalog, our procedure also uses the inverse transformations and inverse distortion solutions to map each pixel of the individual `_flc` exposures into the

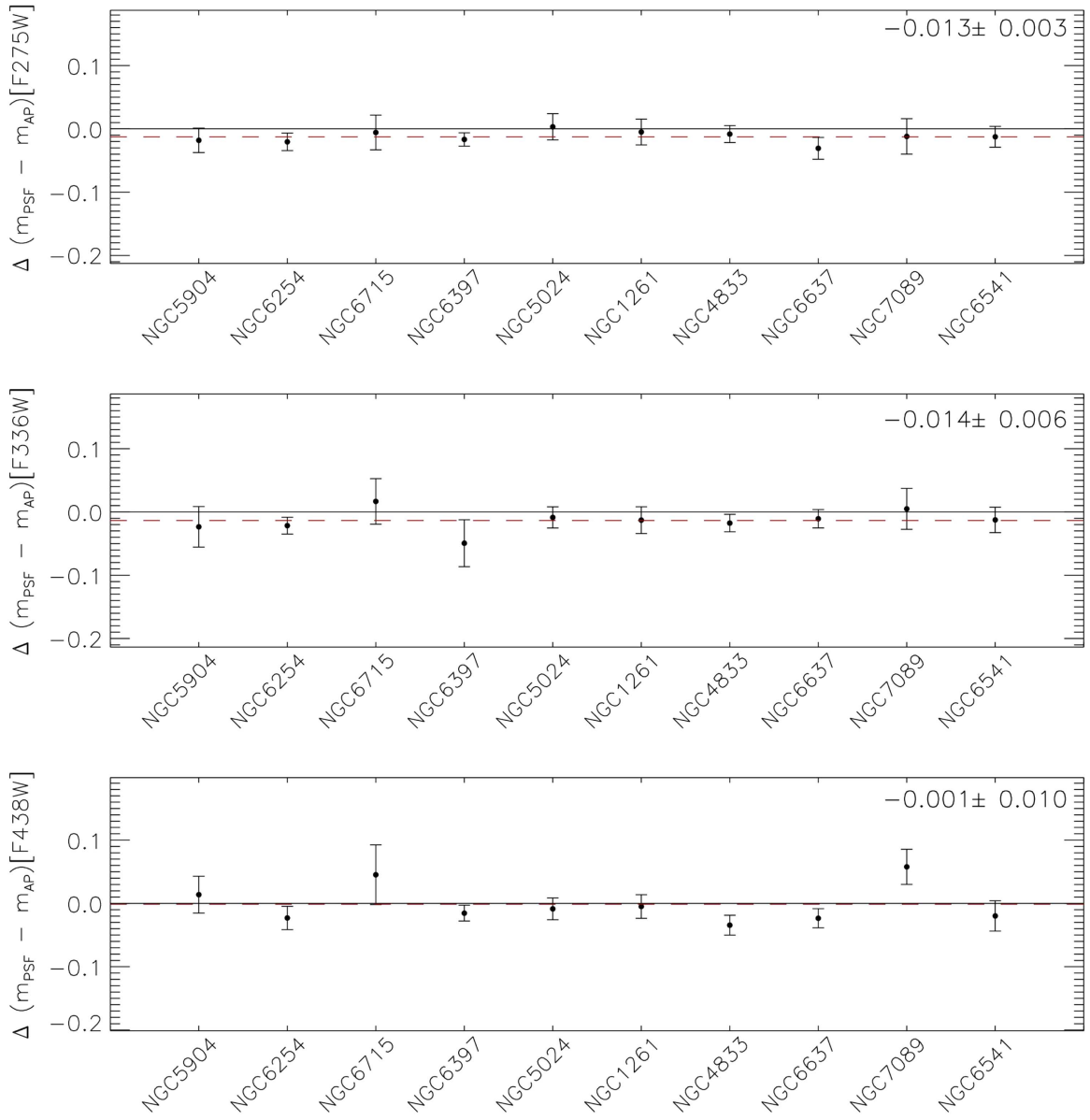

Figure 2. Zeropoint difference between the PSF photometry of the `*_flc` images and the aperture photometry of the `*_drz` images using an aperture of 4.5 pixels (0.″18) in 10 GCs. These zeropoints include the correction for the normalization of our *uvm* magnitudes to 1000 s.

reference frame to generate a representative stack of each band in the ACS GCS frame. These stacks represent the sigma-clipped mean of the nearest pixels from the contributing images and provide a more visual representation of the GO-13297 data in the same frame as the F606W images of the ACS GCS reduction. This should enable users to quickly assess whether particular stars that were missed in this preliminary reduction will be likely to be included when we do the more comprehensive multi-pass final reduction.

These stacks are normalized to correspond to a 1000 s exposure and have the same WCS header information as the GO-10775 images (which have been astrometrically corrected for *HST* guide-star errors to 2MASS). We also place into the image header the pixel location of the cluster center as determined by Goldsbury et al. (2010). Finally, we combined together the F275W, F336W, and F438W images into a single RGB TIFF image for each cluster. This is not useful for science, but may be useful for presentations and highlight the extreme populations. Figure 4 shows the stacked color images for four different clusters.

Eventually, these data will be uploaded to the Mikulski Archive for Space Telescopes[15], but until then they can be accessed at http://www.astro.uda.cl/public_release/globularclusters41.html and at http://groups.dfa.unipd.it/ESPG/treasury.php.

5. SUMMARY

This brief paper describes the preliminary catalog we have generated for the 48 clusters of program GO-13297, the *HST UV Legacy Survey of Galactic Globular Clusters*. We also include in the catalog data taken with previous programs that had the same filter set and scientific goals, for a total of 57 clusters.

[15] http://archive.stsci.edu

Table 2
Catalog Example: NGC 6681

xuv	*yuv*	m275	m336	m438	m275_sig	m336_sig	m438_sig	g2	f2	p2	g3	f3	p3	g4	f4	p4	id_ata	x_ata	y_ata	m606	m814	R.A._ata	Decl._ata	D_x	D_y
0.0	0.0	0.000	0.000	0.000	0.000	0.000	0.000	0	0	0	0	0	0	0	0	0	00001	1103.67	776.87	20.534	19.676	280.83379	−32.32285	0.0	0.0
0.0	0.0	0.000	0.000	0.000	0.000	0.000	0.000	0	0	0	0	0	0	0	0	0	00002	1090.91	984.99	19.944	19.344	280.83400	−32.31995	0.0	0.0
0.0	0.0	0.000	0.000	0.000	0.000	0.000	0.000	0	0	0	0	0	0	0	0	0	00003	1140.71	809.17	21.593	20.817	280.83318	−32.32240	0.0	0.0
0.0	0.0	0.000	0.000	0.000	0.000	0.000	0.000	0	0	0	0	0	0	0	0	0	00004	1167.88	842.12	20.588	19.954	280.83273	−32.32194	0.0	0.0
0.0	0.0	0.000	0.000	0.000	0.000	0.000	0.000	0	0	0	0	0	0	0	0	0	00005	1178.94	850.65	20.542	19.821	280.83255	−32.32182	0.0	0.0
2582.9	3653.3	22.703	21.575	21.787	0.132	0.045	0.083	3	3	4	4	4	4	2	2	2	32554	2582.96	3653.30	20.862	20.198	280.80947	−32.28290	0.0	0.0
2584.3	3661.3	20.582	19.840	20.271	0.027	0.092	0.025	4	4	4	4	4	4	2	2	2	32555	2584.31	3661.32	19.538	18.988	280.80945	−32.28279	0.0	0.0
2586.3	3657.9	21.652	19.917	19.844	0.048	0.033	0.003	4	4	4	4	4	4	2	2	2	32556	2586.52	3657.77	18.735	18.042	280.80941	−32.28284	−0.3	0.2
2582.0	3679.3	20.171	19.560	19.900	0.106	0.013	0.003	4	4	4	4	4	4	2	2	2	32557	2581.94	3679.37	19.158	18.619	280.80949	−32.28254	0.0	0.0
2566.6	3700.3	0.000	0.000	0.000	0.000	0.000	0.000	0	0	4	0	0	4	0	0	2	32558	2566.55	3701.00	26.305	24.527	280.80974	−32.28224	0.1	−0.7
2564.8	3713.2	20.260	19.625	19.924	0.046	0.021	0.015	4	4	4	4	4	4	2	2	2	32559	2564.83	3713.17	19.194	18.655	280.80977	−32.28207	0.0	0.0

Note. Each column description can be summarized as follows: *xuv*, *yuv* are the coordinates transformed into the $0\farcs05$/pix ACS GCS frame, m275 is the VEGAMAG calibrated magnitude in F275W band, m336 is the VEGAMAG calibrated magnitude in F336W band, m438 is the VEGAMAG calibrated magnitude in F438W band, m275_sig is the photometric error of magnitude in F275W filter, m336_sig is the photometric error of magnitude in F336W filter, m438_sig is the photometric error of magnitude in F438W filter, gi, fi, pi are the number of times a star has: a good measurement (g), is found (f), and could have been found (p). The subindex indicates the band of the measurement, F275W ($i = 2$), F336W ($i = 3$), F438W ($i = 4$). id_ata is the identification number of the star in the ACS GCS, x_ata, y_ata are the pixel coordinates of the star in ACS GCS, the coordinates span from 0 to 6000 pixels in each axis, m606, m814 are the VEGAMAG calibrated magnitudes in the ACS GCS in the F606W and F814W filters, RA_ata, DEC_ata are the Right Ascension and Declination in the original ACS GCS, D_x, D_y are the displacements in pixels, in the original ACS GCS axes and pixel size, these are calculated using the ACS GCS, and new WFC3 UV positions as first and second epoch, respectively. The displacements can be converted into mas yr^{-1} proper motions using the formula $\mathrm{PM}_i = (\mathrm{D\_i} \times 50.0)/\Delta\mathrm{Epoch}$, where the ΔEpoch can be found in Table 1 and $i = x, y$. The obtained proper motions can be expressed in units of km s^{-1} using $\mathrm{Vel[km\ s^{-1}]} = 4.74 \times \mathrm{dist[kpc]} \times \mathrm{PM[mas\ yr^{-1}]}$, with dist corresponding to the distance of the cluster from the Sun. We must stress that, while the provided displacements D_i have an accuracy sufficient for cluster-field separation, they are not suited for internal cluster dynamics.

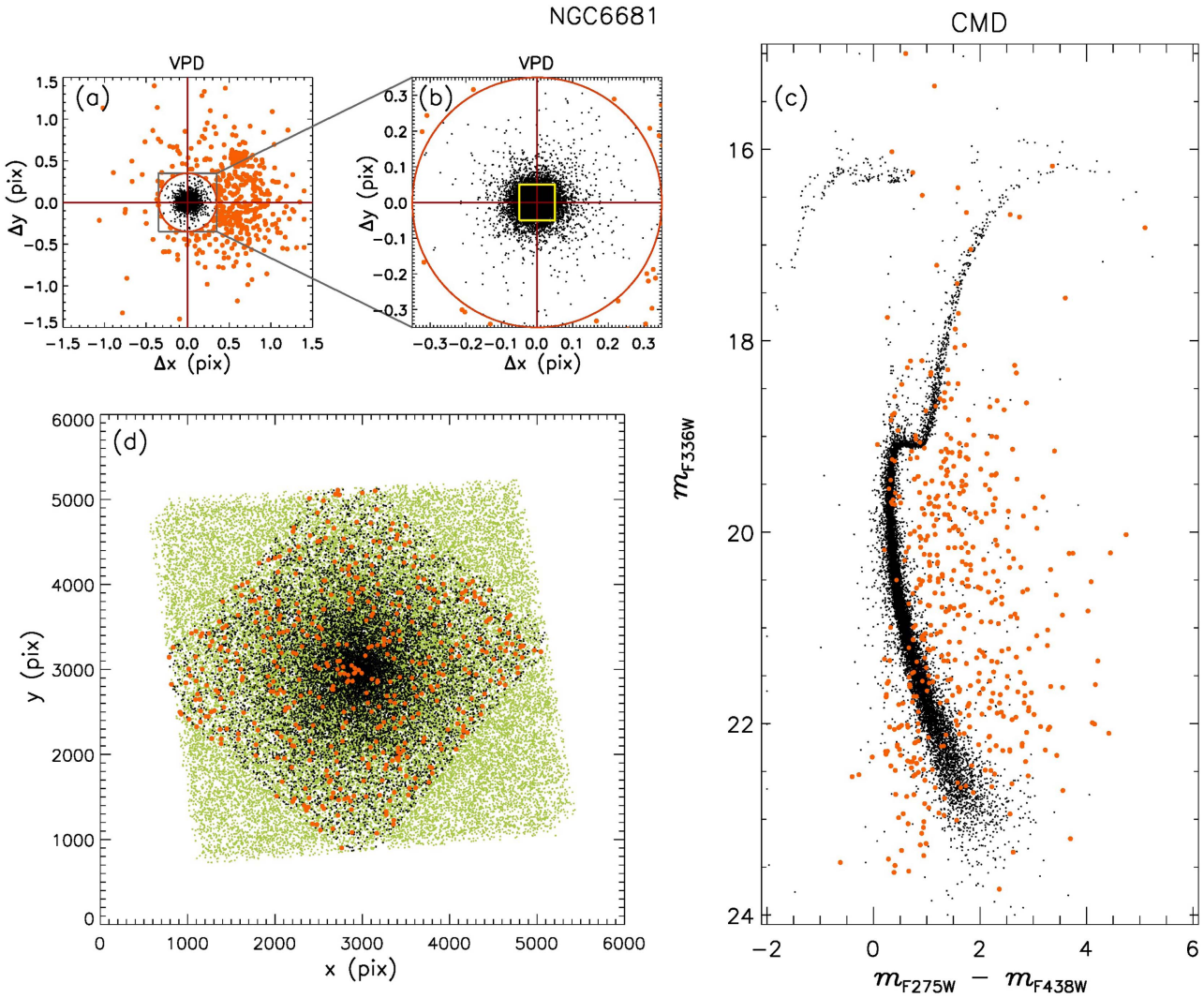

Figure 3. Illustration of the data that our catalog provides for the GC NGC 6681. Panel (a) shows the vector-point diagram (VPD), the displacement (in ACS/WFC pixels), between the 2006 ACS GCS and this catalog (2013–2014)—a ∼7–8 yr time-baseline. We have marked stars with a displacement greater than 0.35 pixel (orange circle) as field stars (orange points) in all plots. Panel (b) is a zoomed version of (a), where the central yellow square represents the reliability of our current crude 2013 positions (0.″005). Panel (c) shows the UV CMD for the complete field, while Panel (d) shows the positions of stars detected in the ACS GCS (light green points) overplotted with those that have also been detected in our WFC3/UVIS UV catalogs (black points).

We ran a one-pass photometry routine on each individual exposure and collated the results against the catalog from GO-10775, the 2006-epoch ACS survey in F606W and F814W. We provide to the community calibrated photometry for each star found in F275W, F336W, and F438W, along with empirical uncertainties and a 2013-epoch position, which can be used for cluster-field separation. Color–color plots from these new catalogs should be particularly effective for identifying stars in different populations to enable spectroscopic follow-up; this is the main reason we sought to make this preliminary catalog available before the final reduction. In addition, we produce a representative stacked image in each band along with a color-composite image.

The data provided here represent the preliminary data products for the survey. The photometry here is different from that in Piotto et al. (2015) in that no customization has been done for each cluster in terms of reddening correction, PSF-modeling, etc. The goal here was to provide a uniform reduction to the community.

Over the next year, we will do a more comprehensive reduction of the data set. Having the entire data set in hand will enable us to construct an improved model of the PSF based on the entire data set, allowing for variations due to focus. Even with such an improved PSF model, we will also construct a perturbation PSF for each exposure so that the stars can be measured as accurately and as consistently as possible. (Faint stars are best measured with smaller apertures, but without a good PSF model, this can introduce systematic errors; to avoid this, here we had to use the same 5×5 pixel aperture for all stars.) We will also improve the distortion solutions and independently evaluate the astrometric and photometric errors that remain after the pixel-based CTE correction.

The final reduction will not be a one-pass procedure as was done here; rather it will use a multi-pass procedure similar to that described in Anderson et al. (2008), though optimized for the three-filter data set that we have here. We will produce new stacks along with subtracted stacks to help users evaluate whether there may be stars that were just below the one-pass finding threshold. We will also perform artificial-star tests to

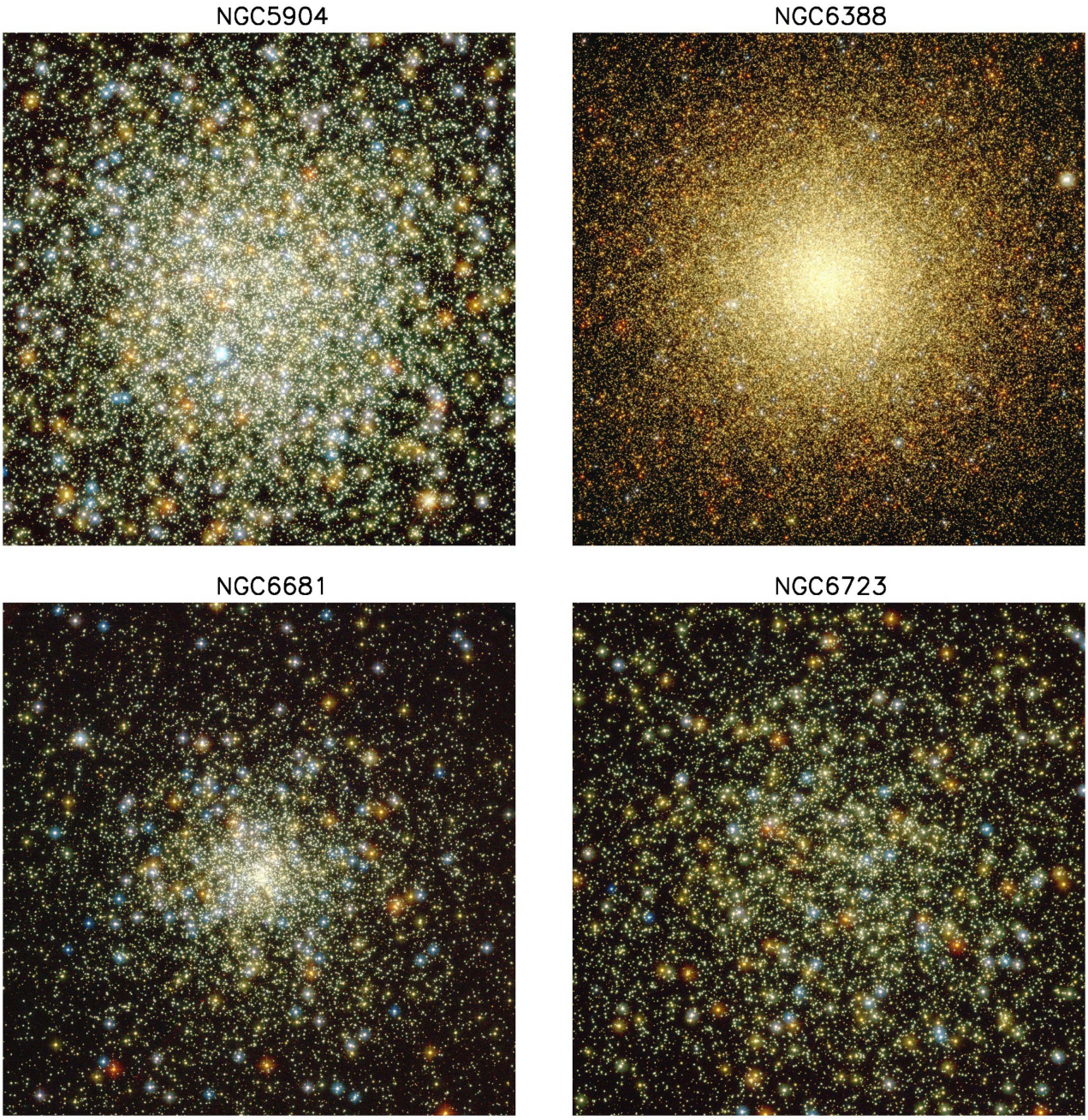

Figure 4. Trichromatic stack images of 4 clusters in our survey NGC 5904, NGC 6388, NGC 6681 and NGC 6723, each image covers a field of 1.′8 × 1.′8.

allow users to evaluate the completeness, photometric errors and possible recovery biases. Finally, we will use the final data set to construct a reddening correction specific to the local neighborhood of each star. These improvements should be made over the course of the next year, with the catalogs released to the community soon thereafter.

M.S., J.A., A.B., A.C., and I.R.K. acknowledge support from STScI grant GO-13297. M.S. acknowledges support from Becas Chile de Postdoctorado en el Extranjero project 74150088. G.P., V.G., S.O., and D.N. acknowledge partial support by the Università degli Studi di Padova Progetto di Ateneo CPDA141214 "Towards understanding complex star formation in Galactic globular clusters" and by INAF under the program PRIN-INAF2014. A.A., S.C., and S.H. recognize partial support by the IAC (grant P301031) and the Ministry of Competitiveness and Innovation of Spain (grant AYA2010-16717). A.P.M. acknowledges support by the Australian Research Council through Discovery Early Career Researcher Award DE150101816.

REFERENCES

Anderson, J. 1997, PhD thesis, Univ. California
Anderson, J., & Bedin, L. 2010, PASP, 122, 1035A
Anderson, J., & King, I. R. 2006, Instrument Science Report ACS 2006-01 (Batimore: STScI)
Anderson, J., Piotto, G., King, I. R., Bedin, L. R., & Guhathakurta, P. 2009, ApJL, 697, L58
Anderson, J., Sarajedini, A., Bedin, L. R., et al. 2008, AJ, 135, 2055
Arp, H. C. 1965, in Galactic Structure, ed. A. Blaauw & M. Schmidt (Chicago, IL: Univ. Chicago Press), 401

Bedin, L. R., Piotto, G., Anderson, J., et al. 2004, ApJL, 605, L125
Bellini, A., Anderson, J., & Bedin, L. R. 2011, PASP, 123, 622
Bellini, A., Anderson, J., van der Marel, R. P., et al. 2014, ApJ, 797, 115
Bellini, A., Piotto, G., Milone, A. P., et al. 2013, ApJ, 765, 32
Carretta, E., Bragaglia, A., Gratton, R. G., Lucatello, S., & Momany, Y. 2007, A&A, 464, 927
Cassisi, S., Salaris, M., Pietrinferni, A., et al. 2008, ApJL, 672, L115
D'Antona, F., Bellazzini, M., Caloi, V., et al. 2005, ApJ, 631, 868
De Angeli, F., Piotto, G., Cassisi, S., et al. 2005, AJ, 130, 116
Di Criscienzo, M., D'Antona, F., Milone, A. P., et al. 2011, MNRAS, 414, 3381D
Djorgovski, S., & King, I. R. 1986, ApJL, 305, L61
Djorgovski, S., & Meylan, G. 1993, in ASP Conf. Ser. 50, Structure and Dynamics of Globular Clusters, ed. S. Djorgovski & G. Meylan (San Francisco, CA: ASP), 325
Dotter, A., Chaboyer, B., Jevremovic, D., et al. 2007, AJ, 134, 376
Dotter, A., Sarajedini, A., Anderson, J., et al. 2010, ApJ, 708, 698
Goldsbury, R., Heyl, J., & Richer, H. 2013, ApJ, 778, 57
Goldsbury, R., Richer, H. B., Anderson, J., et al. 2010, AJ, 140, 1830
Gratton, R. G., Lucatello, S., Bragaglia, A., et al. 2006, A&A, 455, 271
Harris, W. E. 1996, AJ, 112, 1487
Lee, Y.-W., Joo, J.-M., Sohn, Y.-J., et al. 1999, Natur, 402, 55
Marín-Franch, A. 2009, ApJ, 694, 1498
Marino, A. F., Milone, A. P., Piotto, G., et al. 2009, A&A, 505, 1099
Marino, A. F., Villanova, S., Piotto, G., et al. 2008, A&A, 490, 625
Milone, A. P., Bedin, L. R., Piotto, G., et al. 2008, ApJ, 673, 241
Milone, A. P., Marino, A. F., Dotter, A., et al. 2014, ApJ, 785, 21
Milone, A. P., Marino, A. F., Piotto, G., et al. 2013, ApJ, 767, 120
Milone, A. P., Piotto, G., Bedin, L. R., et al. 2012, ApJ, 744, 58
Milone, A. P., Piotto, G., King, I. R., et al. 2010, ApJ, 709, 1183
Paust, N. E. Q., Reid, I. N., Piotto, G., et al. 2010, AJ, 139, 476
Piotto, G., Bedin, L. R., Anderson, J., et al. 2007, ApJL, 661, L53
Piotto, G., King, I. R., Djorgovski, S. G., et al. 2002, A&A, 391, 945
Piotto, G., Milone, A. P., Anderson, J., et al. 2012, ApJ, 760, 39
Piotto, G., Milone, A. P., Bedin, L. R., et al. 2015, AJ, 149, 91
Piotto, G., Milone, A. P., Marino, A. F., et al. 2013, ApJ, 775, 15
Rosenberg, A., Piotto, G., Saviane, I., & Aparicio, A. 2000, A&AS, 144, 5
Sarajedini, A., Bedin, L. R., Chaboyer, B., et al. 2007, AJ, 133, 1658
Shapley, H. 1930, Stars Clusters (New York: McGraw-Hill)
Shapley, H. 1918, Contributions from the Mount Wilson Observatory, 157, 1S
Siegel, M. H., Dotter, A., Majewski, S. R., et al. 2007, ApJ, 667, 57
VandenBerg, D. A., Brogaard, K., Leaman, R., & Casagrande, L. 2013, ApJ, 775, 134
Webbink, R. F. 1985, in IAU Symp. 113, Dynamics of Stars Clusters, ed. J. Goodman & P. Hut (Dordrecht: Reidel), 541